Structural Dynamics of an Actin Spring

L. Mahadevan,[†‡*] C. S. Riera,[†] and Jennifer H. Shin[§]
[†]School of Engineering and Applied Sciences, Harvard University, Cambridge, Massachusetts; [‡]Department of Organismic and Evolutionary Biology, Harvard University, Cambridge, Massachusetts; and [§]Department of Bio and Brain Engineering, and Department of Mechanical Engineering, Korea Advanced Institute of Science and Technology, Daejeon, Republic of Korea

ABSTRACT Actin-based motility in cells is usually associated with either polymerization/depolymerization in the presence of cross-linkers or contractility in the presence of myosin motors. Here, we focus on a third distinct mechanism involving actin in motility, seen in the dynamics of an active actin spring that powers the acrosomal reaction of the horseshoe crab (*Limulus polyphemus*) sperm. During this process, a 60-μm bent and twisted bundle of cross-linked actin uncoils and becomes straight in a few seconds in the presence of Ca^{2+}. This straightening, which occurs at a constant velocity, allows the acrosome to forcefully penetrate the egg. Synthesizing ultrastructural information with the kinetics, energetics, and imaging of calcium binding allows us to construct a dynamical theory for this mechanochemical engine consistent with our experimental observations. It also illuminates the general mechanism by which energy may be stored in conformational changes and released cooperatively in ordered macromolecular assemblies.

INTRODUCTION AND EXPERIMENTAL OBSERVATIONS

The dynamics of conformational change in crystalline biopolymers is of importance in a number of subcellular processes such as self-assembly, polymorphism, switching, and folding. Examples of protein polymorphism arise in bacterial flagella (1,2), which can exist in a range of helical states; microtubules that exhibit dynamic instability (3); virus shells that inflate, facet, and thin as they mature (4); phage viruses that drill into their bacterial hosts (5); and the collective dynamics of allosteric transitions in large protein assemblies (6). In each of these examples, a unit cell of the macromolecular assembly, which consists of a large number of identical subunits, can exist in multiple states. Thus, even a small conformational change at the level of a subunit leads to a large amplification at the mesoscopic scale simply due to the multiplication of this change by the number of subunits, if the structural architecture permits this. From a dynamical perspective, a natural question is how these conformational changes occur: are they simultaneous over the entire assembly or do they propagate along it? Indeed, this general question can be asked of any large assembly, including that of protein misfolding, where large ordered aggregates are often polymorphic.

Here, we consider an example of such a conformational change in eukaryotes that is particularly well studied from a structural and biochemical perspective and thus amenable to a quantitative physical approach. In the acrosomal reaction of the *Limulus polyphemus* (horseshoe crab or Xiphosura), the sperm cell swims up to the egg, where there is an abundance of Ca^{2+} ions, after which a 60-μm-long twisted, bent, and coiled bundle of protein (24–68 nm in radius) extends from the anterior of the sperm cell, penetrates the egg, and starts the fertilization process. This irreversible reaction converts the coil to a straight rod termed true discharge (TD) (Fig. 1, *a* and *b*). The bundle is composed of just three proteins, cytoskeletal actin, a tight dimeric cross-linker scruin, and the calcium-binding protein calmodulin, in a stoichiometric ratio of 1:1:1 (7).

A simple way of activating the reaction is to use a combination of sea water and calcium ionophores (see Appendix: Methods and Materials), which allows us to quantify the extruded length of the actin bundle as a function of time (8). We see that the velocity is constant when triggered by calcium ionophores (Fig. 1, *d* and *e*)—something hinted at by Tilney and deRosier (10) but never measured quantitatively until now. We also note that the velocity varies substantially (2–37 μm/s), increasing with temperature. Our primary goal is to explain this constant-velocity extrusion using knowledge of the structure and biochemistry of the bundle, which forms a minimal system in which to study the collective dynamics of protein conformation change. An understanding of the temperature dependence will then follow, albeit at a qualitative level.

In the next section, we describe the structural basis for our model, quantify the coupling between untwisting and extension of the bundle, and describe the biochemical basis for our model, focusing in particular on the role of calcium in the acrosomal reaction. We then introduce a mathematical model for the dynamics of the acrosome reaction and use it to study the evolution of the different processes. We conclude with a brief discussion of our results and generalizations of our model to other polymorphic systems.

Submitted September 24, 2010, and accepted for publication December 2, 2010.

*Correspondence: lm@seas.harvard.edu

Editor: Charles W. Wolgemuth.

0006-3495/11/02/0839/6 $2.00

doi: 10.1016/j.bpj.2010.12.3743

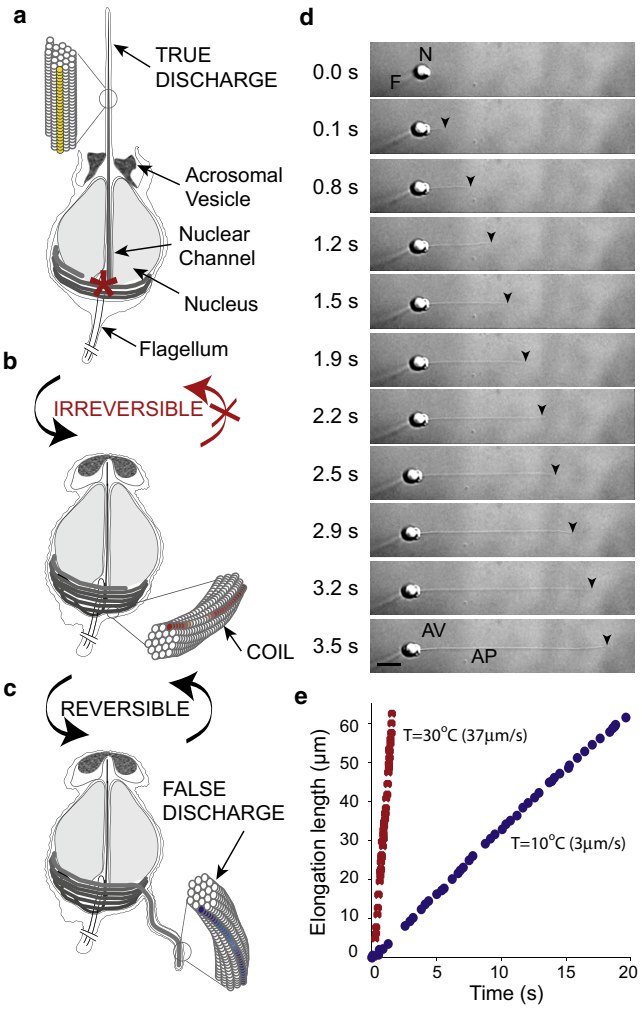

FIGURE 1 (*A*) The geometry and dynamics of the acrosomal reaction. (*a–c*) Geometry (according to DeRosier et al. (10)) shows that in the presence of Ca^{2+}, the bundle switches irreversibly from coil (*b*) to TD (*a*), whereas the reaction from coil to FD (*c*) occurs spontaneously and reversibly. The super-twisting of the actin filaments has opposite chirality in the coil and FD, as shown by the colored strand; the TD exhibits no super-twisting. (*d*) The tip moves at a constant velocity as the acrosomal process is extruded out of the acrosomal vesicle due to the propagation of an untwisting front. (N: nucleus, F: flagellum). Scale bar, 5 μm. (*e*) Extrusion occurs at constant speed. The two traces correspond to extrusion at 10°C (3 μm/s) and 30°C (37 μm/s).

STRUCTURE AND BIOCHEMISTRY

Structurally, the bundle can exist in three different states (Fig. 1, *a–c*). In its coiled state, the bundle is made of a helically structured array of actin filaments that are cross-linked by the protein scruin. This helical arrangement of the bundle is tightly coupled to the conformation of individual actin filaments, each of which has a small overtwist of 0.23°/actin subunit (5 nm in size) relative to the natural chiral structure of an actin filament in the TD (9). Occasionally, the bundle uncoils from its posterior end leading to the so-called false discharge (FD), a reaction that does not require calcium and is reversible and controllable (10,11) (Fig. 1, *b* and *c*). In the FD, the filaments are undertwisted by 0.21°/actin subunit relative to those in the TD (10). When calcium is bound to the coil, the bundle becomes straight and there is no net twist in the actin filaments relative to each other. In all three states of the bundle, the filaments remain cross-linked, but their relative arrangements are different, so that there is a strong similarity of the system to certain crystals where the different possible packing arrangements lead to solid-solid displacive phase transitions (12). There are no known motor proteins in the assembly, and furthermore, there is no growth or shrinkage of the bundle during the reaction. Thus, we see here a third distinct form of actin-based motility similar to a mechanochemical spring with just three components, quite different from polymerization engines (13) based on growth/shrinkage and musclelike motility, where myosin motors move on actin tracks (13).

In its coiled state, the bundle is polygonal, with straight sides separated by a set of periodically spaced, sharply bent elbows (kinks) forming a regular 14-gon (Fig. 2 *a*); along each arm, the actin filaments are supertwisted by ~60° (14). To understand the kinks, we note that for strong cross-links, i.e., a highly energetic interaction between the scruin-decorated filaments, the best possible way to bend a bundle involves using a series of regularly spaced kinks separated by almost straight sections, rather than having a smoothly bent bundle, as explained qualitatively by DeRosier et al. (10) and calculated theoretically by Cohen and Mahadevan (15). In going from the coil to the TD, the bundle rotates through an angle of 60°/arm, leading to a drilling motion (Fig. 2 *b*) and a simultaneous global elongation; during this process, the actual length of the bundle does not change. The kinks help to convert twist in the arms of the bundle into extension but are otherwise passive and do not themselves have to participate in the uncoiling. Indeed, they can persist without melting even after the reaction is complete (Fig. 2 *c*). This observation shows that we can separate the microscopic mechanism of untwisting of the filaments in the bundle from the melting of the kinks, thus simplifying our analysis later.

To quantify the conversion of twist to extension in the bundle, we consider that a straight segment of the twisted bundle of length l lies in a plane. When this segment untwists by a total angle ϕ, the bundle undergoes a global conformation change; for example, if $\phi = \pi$, the kinked, coiled bundle straightens as each segment of the bundle untwists, eventually yielding a zig-zag, extended bundle that lies in the plane. In more general terms, the untwisting leads to a kinked helix, whose end-to-end distance can be computed in terms of the twist angle ϕ and the kink angle θ. For the bundle, we can decompose this process into a rotation about the tangent to the segment followed by a rotation about the local binormal and finally a translation of l along the tangent axis to shift the segment by its own length. Thus,

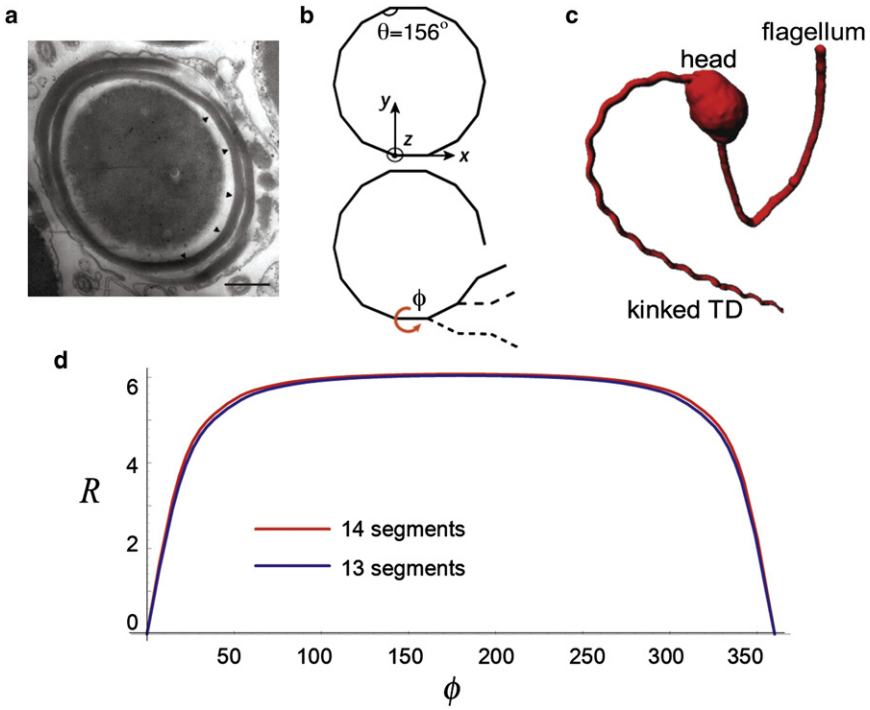

FIGURE 2 Mechanism of converting twist to extension. (*a*) Electron micrograph of a coil shows a polygonal loop with straight sides separated by a set of periodically spaced sharply bent elbows (kinks) forming a regular 14-gon. Scale bar, 5 μm. (*b*) In going from the coil to the TD, the bundle has to rotate through an angle of ϕ=60o at each arm. As the untwisting front propagates along the bundle, it extends out eventually forming a zig-zag shape. (*c*) The zig- zag kinks play a passive role in the conversion of twist to extension and may persist after the reaction is complete. (Images in *a* and *b* were originally published in Shin et al. (17).) (*d*) The two curves correspond to the total elongation after the untwisting of one loop for 13 (*blue*) and 14 (*red*) arms. For an even number of arms, the elongation is less sensitive to the total angle of twist per arm.

the total elongation after the untwisting of one loop of the bundle of radius R with n kinks is

$$L = \sum_{i=0}^{n-1} \sqrt{\left(\left(r_z(\pi-\theta)r_x(\phi)^i\right)r_z(\pi-\theta)l\right)^2}, \qquad (1)$$

where r_z and r_x represent rotation about the z and x axes, respectively, θ is the kink angle, ϕ is the twist angle, and l is the length of the straight segment.

As shown in Fig. 2 *d*, the elongation is close to the maximum for a large range of the total twist angle/segment, ϕ, which enables some variations in the length and twist of each arm without being inefficient in conversion of twist to extension. We note parenthetically that this very clever mechanism for converting twist to extension is likely to be found elsewhere in biology, and is certainly useful in thinking about engineering nanodevices.

Having characterized the geometry of the bundle as it untwists and thus uncoils, we now turn to the role of Ca^{2+}, which is known to be responsible for the change in the conformation of scruin (16) since the scruin dimer is tightly attached to the calcium-binding protein calmodulin. Indeed, structural and biochemical studies of scruin show that it acts like a molecular latch that holds the actin filaments in their twisted conformation until calcium binds to calmodulin, whereupon scruin relaxes to an open structure leading to the untwisting of the actin bundle. From an energetic perspective, our earlier work (17) showed that the elastic potential energy stored in the bundle is two orders of magnitude larger than the chemical energy of Ca^{2+} binding to the bundle. Thus, Ca^{2+} binding leads to a change in the effective energy landscape of the system, but it does not directly control the spatiotemporal dynamics of the reaction. This leads us to suggest the following model for the mechanism at work in this mechanochemical engine: 1), Ca^{2+} binds to scruin; 2), the scruin-actin interactions are changed ever so subtly; 3), a small region of the coil begins to untwist, since the interaction between neighboring actin filaments is mediated by scruin, which decorates them; 4), this untwisting deforms the bundle of actin without completely un-cross-linking it in the binding region and is driven by the potential energy difference between the coil and true states of the bundle; and 5), Ca^{2+} binds to calmodulin further along and releases the twisted state, leading to the propagation of a front of twisting that traverses along the bundle. Since ion binding is typically a fast event relative to protein sliding, we expect that the rate-limiting step in the dynamics of untwisting and force generation is the slow cooperative untwisting of the filaments (18,19).

Taken together, these observations and calculations suggest that we can understand the dynamics of the acrosomal reaction by focusing on a minimal picture of an untwisting actin bundle in the presence of calcium; the kinks then allow for a transformation of twist to bend and thence to extension.

MATHEMATICAL MODEL AND ANALYSIS

As shown in Fig. 3, the actin bundle can exist in two locally stable states, the coil and the FD in the absence of calcium.

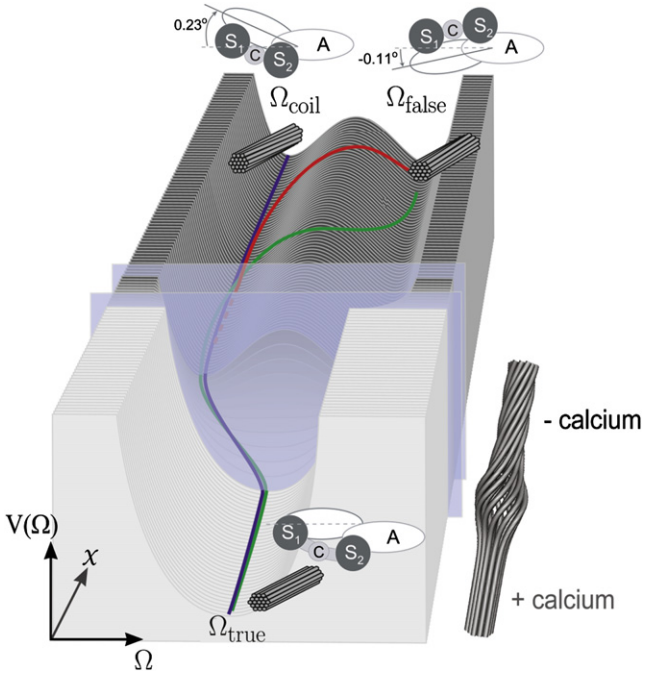

FIGURE 3 Mechanochemistry of the acrosomal reaction. In the absence of calcium, the FD and the coil are locally stable, whereas the TD doesn't exist. Due to the molecular chirality of actin, the coil and FD states are not identical but interconvertible, as observed in experiments. When the bundle binds to calcium, the TD state disappears (*red line*), so that the reaction occurs spontaneously and an untwisting front propagates from the coil to the FD state. The natural order parameter in this system is the twisting strain $\Omega = \phi_x$, and A, C, S_1, and S_2 correspond to the actin, the calmodulin, and the two scruin domains, respectively.

However, once the calcium binds to calmodulin, the scruin dimer changes its conformation so that the actin filaments untwist into a stable straight true discharge. Since the relative twisting of the filaments is what characterizes these states, we define the twisting strain in the actin bundle as $\Omega = \phi_x$,where $\phi(x,t)$ is the twist of individual filaments relative to the center line of the bundle at a location x along the contour of the bundle measured from the tip, and $(.)_x = \partial_x(.)$. The coil and FD states are approximately symmetrically located relative to the state $\Omega = 0$ which is locally unstable when there is no calcium. However, since the actin bundle is constituted of chiral actin filaments, we can expect that a weak signature persists, leading to an asymmetry between the coil and FD, so that $\Omega_{\text{coil}} \neq \Omega_{\text{false}}$. Once calcium binds to the bundle, the potential changes from having two minima to just one minimum corresponding to the true discharge $\Omega = 0$ (Fig. 3). Then, a minimal model for the energy, E, that incorporates these features may be written as a function of the twist strain, Ω, via a Landau-type model of the type used to describe protein polymorphisms in bacterial flagella (1,20):

$$E = \int \left[V(\Omega) + \frac{Cr^2}{2}\Omega_x^2 \right] dx, \tag{2}$$

where the twist-gradient coefficient ,Cr^2, with C related to the torsional rigidity and r the radius of the bundle, controls the width of the front (20) connecting the two states just as gradient terms set front widths in problems involving phase transitions. Here, the potential $V(\Omega) = -\alpha\Omega^2/2 + \beta\Omega^4/4 + \delta\Omega$ in the absence of calcium, but it changes when calcium binds to the bundle, so that α and β might themselves be functions of time. If r is the radius of the bundle, frictional torque/unit length of the bundle due to the rate of change of twist of the filaments scales as $\mu_i \int r\varphi_{xt} r dA \sim \mu_i r^4 \varphi_{xt}$, where μ_i is the viscosity characterizing the protein-protein interaction between the filaments and dominates the torque due to the rotation of the bundle inside the nuclear channel as well as the rotation of the bundle in the ambient fluid outside the cell. We can see this as follows: if Δr is the clearance between the bundle and the channel and μ the viscosity of the fluid inside the channel, then the channel torque scales as $\mu r^4 \phi_t/\Delta r$. This contribution is dominated by the frictional interactions between scruin-decorated actin filaments as they slide past each other, since $\mu_i r^4 \varphi_{xt}/(\mu r^4/\Delta r \varphi_t) \sim \mu_i \Delta r/\mu r \sim 10^2$, where we have used the parameter values $\Delta r/r \sim 10$ nm/100 nm and $\mu_i/\mu \sim 10$ Pa·s/10^{-2} Pa·s based on estimates of protein friction (18,19), and the effective viscosity of the filtered cytoplasm is assumed to be ~10 times that of water. Therefore, the dynamics of untwisting will be rate-limited by protein friction rather than the kinetics of calcium-binding. Local torque balance then leads to the following evolution equation for the twisting strain:

$$\eta\Omega_{xt} = -\partial_x \frac{\delta E}{\delta \Omega} = -\partial_x \left[\frac{\delta V}{\delta \Omega} - Cr^2 \Omega_{xx} \right], \tag{3}$$

with $\eta = \mu_i r^4$ the effective internal friction coefficient. We note that this dynamical model is different from that introduced by Goldstein and colleagues (20,21) to explain flagellar polymorphisms, where a frictional resistance proportional to the speed of rotation in the ambient fluid, given by $\zeta\Omega_t$, is used on the lefthand side of Eq. 3. This leads to a Cahn-Hilliard-like system, which is known to not support a constant velocity front (22). However, if the frictional dissipation is primarily due to local protein friction, associated with a dependence on the strain rate as in Eq. 3, one gets constant velocity fronts as we now show.

Integrating Eq. 3 once with the condition of zero flux of twist ($\Omega_x = 0$) far from the front yields a Ginzburg-Landau-like equation for the evolution of the twisting strain:

$$\eta\Omega_t = -\frac{\delta V}{\delta \Omega} + Cr^2 \Omega_{xx}. \tag{4}$$

The untwisting in the bundle occurs where the bundle switches from the bent-twisted state to the untwisted state and is rate-limited by the dynamics of the protein friction, as discussed earlier. Once calcium binds to the bundle, the

double-well potential switches to a simple single-well potential given by $V = C\Omega^2/2$; we assume that the binding of this small molecule is rapid relative to the cooperative untwisting of the macromolecular assembly. Then, the dynamical equation for the relaxation of twist reads

$$\eta\Omega_t = -C\Omega + Cr^2\Omega_{xx}, \tag{5}$$

with boundary conditions $\Omega|_{x\to+\infty} = \Omega_x = 0$ and $\Omega_x/\Omega|_{x=0} = b$ where the calcium binds. Looking for an untwisting-front solution that propagates at constant velocity v of the form $\Omega = \Omega(0)e^{b(x+vt)}$ yields the expression

$$v = \frac{-C + Cr^2b^2}{\eta b}. \tag{6}$$

Using the experimentally measured values of the elastic modulus of the bundle (23), $E \sim 2$ GPa, the average bundle radius, $r \sim 5 \times 10^{-8}$ m, the twisting stiffness, $C \sim Er^4$, the coil twisting strain, $\Omega_c \sim 1.5 \times 10^6$ m^{-1}, along with an estimate of the protein viscosity, $\mu_i \sim 1$ Pa·s, so that the twisting viscosity is $\eta \sim \mu_i r^4$, we are left with one unknown parameter, b, in the model. Using the maximum extrusion velocity obtained experimentally, $v_e \sim 40 \times 10^{-6}$ m·s^{-1} (Fig. 1 *e*), implies that the untwisting velocity, which scales with the extrusion velocity, is $v \sim 10 \times 10^{-6}$ m·s^{-1}, according to Eq. 1, so that we can solve Eq. 6 to obtain $b \sim 4.10^7$ m^{-1} and the front width $\Omega/\Omega_x \sim 1/b \sim 50$ nm is comparable to the radius of the bundle, i.e., the front is strongly localized, a reasonable result that is consistent with other systems that exhibit localized fronts of conformation change (6). This estimate can also be seen immediately by noting that the solution of Eq. 6 is given by $br \sim 1$, since $\mu v/Er \sim 1$. Recent calcium imaging experiments (11) show that there is clearly an untwisting front, which can be stopped and restarted by chelating and reintroducing calcium in the environment of the cell. Although there is as yet no direct structural evidence for the localization of the front to the region where the coil switches from its coiled to its straight state at the entrance to the nuclear tunnel, the ability to control the progress of the reaction is strongly suggestive of this scenario.

We now turn briefly to the temperature dependence of the speed of extrusion (Fig. 1 *e*). Since the rate of a chemical reaction depends on temperature via an Arrhenius factor, one might expect its role to be relatively weak given the modest changes in temperature. However, since adhesive and frictional interactions between the sliding filaments also depend on the elasticity of the soft polymeric elements, which have a linear dependence on temperature, this might explain the trends seen. For example, in Eq. 6, we see that the speed depends linearly on the twisting stiffness of the bundle, consistent with this trend. We also observe that the variance in the speed increases with temperature, although the reasons for this are not entirely clear.

The spontaneous reversible transition between the coil and the FD does not require calcium. For the double-well potential $V(\Omega) = -\Omega^{(s)^2}\Omega^2/2 + \Omega^4/4 + \delta\Omega$, with $\Omega \approx \pm\Omega^{(s)}$ being the twist strain associated with the coil/FDs, the symmetry-breaking term characterizing the small energetic difference between the coil and FD is $\delta\Omega$. When $\delta = 0$, the front connecting the two stable states is stationary, with a shape given by the solution of the equation

$$\Omega_s^2\Omega - \Omega^3 + Cr^2\Omega_{xx} = 0, \tag{7}$$

which yields the form of the stationary twisting front $\Omega_0(x) = \Omega_s \tanh\sqrt{\Omega_s^2/2Cr^2}\,x$. When $\delta \neq 0$, the front speed is found by computing the first-order solvability condition (in δ) (22) and yields

$$v = \frac{3\sqrt{Cr^2}}{2\sqrt{2\Omega_S^2\eta}}\Delta V, \tag{8}$$

i.e., the front velocity is linearly proportional to the difference of potential energy between the two states, $\Delta V = -2\Omega_s\delta$. However, to create such a front, the bundle needs to overcome the barrier associated with a nucleation solution by creating a length of FD (22), $l_{FD} \sim 1/\sqrt{2}(3\log(\Omega_s) + \log(8/\delta))$. These observations are also qualitatively consistent with experiments that can evoke a very slow false-discharge reaction via an osmotic stress (11) once it is larger than a critical value. To understand the observation that the FD first retracts into the cell from the rear before uncoiling from the head, we note that an asymmetry in the potential energy makes it harder to twist the bundle in the direction of the twist of the FD than in the direction of the coiled state when the calcium binds to the bundle. Then the energy of the FD is much higher than the barrier of nucleation between the false and coiled states and thus naturally leads to the coiled state being converted into the true state.

DISCUSSION

Our analysis of the acrosome reaction in the *Limulus* brings together the structural, biochemical, and biophysical aspects of the problem, shows how molecular scales couple to the mesoscopic function and allows us to quantify 1), the sequential binding of calcium as the trigger for the reaction, consistent with recent experiments (11) showing that calcium chealation and reintroduction allow us to control the reaction; 2), the constant velocity dynamics of the mechanical front as the rate-limiting step in determining the dynamics of uncoiling and force generation; 3), the reversible FD-coil reaction, which can occur spontaneously; 4), the transition between FD and TD via the intermediary coil; and 5), the role of calcium in the process, which although necessary to start and maintain the reaction does not provide the energy for extrusion, which comes from the stored conformational energy in the twisted bundle.

The horseshoe crab acrosomal process illustrates how conformational changes in proteins can lead to allosteric amplifications acting as a driving force for dynamic processes such as motility. More generally, this points to a general formalism for the dynamics of protein polymorphism due to the combination of slender geometry and the relatively weak forces holding macromolecular assemblies together. The driving power behind these conformational changes is typically balanced by the dissipation at the macromolecular level in the local neighborhood of a front, and generically leads to extrusion at constant velocity.

Our study is but one more example of how polymorphic transitions arise in a variety of situations in molecular settings including viruses (4,5), bacterial flagella (20,21,24), spirochetes (25), and more generally in allosteric interactions (6). Given these quantitative approaches to protein polymorphisms in various different settings, which account for both the complex structural interactions and the internal dynamics of sliding and shearing that accompany these changes, two interesting questions arise: 1), what are the general principles behind their assembly and dynamics? and 2), how easy or difficult are they to evolve?

In the specific context of the acrosomal process, how these conformational strains are first trapped during the assembly of the bundle is a question raised a while ago by Tilney (7). One possibility, suggested by the disorder in actin twist that has been long documented, is that when scruin binds to actin, it functions as a torsional Brownian ratchet, building twist into the assembly. Studies of assembly in vitro using TD bundles as nuclei for growth does not lead to twisted bundles, but by studying partially assembled bundles in vivo in developing sperm cells, we may get a clue to how strain energy is built into these assemblies.

APPENDIX: MATERIALS AND METHODS

Sperm cells were collected from male crabs and washed twice in artificial sea water (ASW) (in mM, 423 NaCl, 9 KCl, 9.27 $CaCl_2$, 22.94 $MgCl_2$, 25.5 $MgSO_4$, 2.15 $NaHCO_3$, and 10 Tris, pH adjusted to 7.9–8.0). The sample was then diluted 1:1000 with ASW and injected into a flow chamber constructed from coverslips and double-sided adhesive tape to conduct the experiments. To immobilize the cells, the bottom coverslip was first treated with a 2% (v/v in acetone) BIOBOND nonspecific adhesive solution and then rinsed with water. The TD reaction was induced by adding calcium ionophore A23187 (1 mg/ml in dimethyl sulfoxide; 21045, Sigma Aldrich, St. Louis, MO) diluted 1:10 in 25 mM$CaCl_2$ ASW. The FD extension was induced by adding either FD reaction buffer (0.1% Triton X-100, 0.1 mM EDTA, 3 mM MgCl2, and 30 mM Tris, pH 8 (4°C)) or salty ASW with increased NaCl. All experiments were performed at room temperature with a Nikon TE-3000 inverted microscope with a NA 1.4 100× oil-immersion objective. Video was recorded with a Dage MTI CCD100 camera, and digitized for tracking with a PC. Individual extension profiles were visually tracked using software provided by Photron Cameras (San Diego, CA).

The authors thank P. Matsudaira for encouragement through the duration of this project and M. Argentina for discussions on the general formalism of front propagation.

REFERENCES

1. Oosawa, F., and S. Asakura. 1975. Thermodynamics of the Polymerization of Protein. Academic Press, New York.
2. Hotani, H. 1976. Light microscope study of mixed helices in reconstituted *Salmonella* flagella. *J. Mol. Biol.* 106:151–166.
3. Mahadevan, L., and T. J. Mitchison. 2005. Cell biology: powerful curves. *Nature.* 435:895–897.
4. Johnson, J. E., and J. A. Speir. 1997. Quasi-equivalent viruses: a paradigm for protein assemblies. *J. Mol. Biol.* 269:665–675.
5. Moody, M. F. 1973. Sheath of bacteriophage T4. 3. Contraction mechanism deduced from partially contracted sheaths. *J. Mol. Biol.* 80:613–635.
6. Bray, D., and T. Duke. 2003. Conformatonal spread: the propagation of allosteric states in large multiprotein complexes. *Annu. Rev. Biophys. Biomol. Struct.* 33:53–73.
7. Tilney, L. G. 1975. Actin filaments in the acrosomal reaction of *Limulus* sperm. Motion generated by alterations in the packing of the filaments. *J. Cell Biol.* 64:289–310.
8. Shin, J. H., B. K. Tam, …, P. Matsudaira. 2007. Force of an actin spring. *Biophys. J.* 92:3729–3733.
9. Sherman, M. B., J. Jakana, …, M. F. Schmid. 1999. The three-dimensional structure of the *Limulus* acrosomal process: a dynamic actin bundle. *J. Mol. Biol.* 294:139–149.
10. DeRosier, D. J., L. G. Tilney, …, P. Frankl. 1982. A change in twist of actin provides the force for the extension of the acrosomal process in *Limulus* sperm: the false-discharge reaction. *J. Cell Biol.* 93:324–337.
11. Tam, B. K., J. H. Shin, …, L. Mahadevan. 2009. Calcium regulation of an actin spring. *Biophys. J.* 97:1125–1129.
12. Nabarro, F. R. N. 1993. Theory of Crystal Dislocations. Dover, New York.
13. Bray, D. 2000. Cell Movements, 2nd ed. Garland, New York.
14. DeRosier, D., L. Tilney, and P. Flicker. 1980. A change in the twist of the actin-containing filaments occurs during the extension of the acrosomal process in *Limulus* sperm. *J. Mol. Biol.* 137:375–389.
15. Cohen, A. E., and L. Mahadevan. 2003. Kinks, rings, and rackets in filamentous structures. *Proc. Natl. Acad. Sci. USA.* 100:12141–12146.
16. Sanders, M. C., M. Way, …, P. Matsudaira. 1996. Characterization of the actin cross-linking properties of the scruin-calmodulin complex from the acrosomal process of *Limulus* sperm. *J. Biol. Chem.* 271:2651–2657.
17. Shin, J. H., L. Mahadevan, …, P. Matsudaira. 2003. Stored elastic energy powers the 60-microm extension of the *Limulus polyphemus* sperm actin bundle. *J. Cell Biol.* 162:1183–1188.
18. Tawada, K., and K. Sekimoto. 1991. Protein friction exerted by motor enzymes through a weak-binding interaction. *J. Theor. Biol.* 150:193–200.
19. Bormuth, V., V. Varga, …, E. Schäffer. 2009. Protein friction limits diffusive and directed movements of kinesin motors on microtubules. *Science.* 325:870–873.
20. Goldstein, R. E., A. Goriely, …, C. W. Wolgemuth. 2000. Bistable helices. *Phys. Rev. Lett.* 84:1631–1634.
21. Coombs, D., G. Huber, …, R. E. Goldstein. 2002. Periodic chirality transformations propagating on bacterial flagella. *Phys. Rev. Lett.* 89:118102.
22. van Saarloos, W. 2003. Front propagation into unstable states. *Phys. Rep.* 386:219–229.
23. Shin, J. H., L. Mahadevan, …, P. Matsudaira. 2004. Bending stiffness of a crystalline actin bundle. *J. Mol. Biol.* 337:255–261.
24. Srigiriraju, S. V., and T. R. Powers. 2006. Model for polymorphic transitions in bacterial flagella. *Phys. Rev. E Stat. Nonlin. Soft Matter Phys.* 73:011902.
25. Kan, W., and C. W. Wolgemuth. 2007. The shape and dynamics of the *Leptospiraceae*. *Biophys. J.* 93:54–61.